Communication

In situ Observation of Calcium Oxide Treatment of Inclusions in Molten Steel by Confocal Microscopy

BHARAT KHURANA, STEPHEN SPOONER, M.B.V. RAO, GOUR GOPAL ROY, and PRAKASH SRIRANGAM

Calcium treatment of aluminum killed steel was observed *in situ* using high-temperature confocal scanning laser microscope (HT-CSLM). This technique along with a novel experimental design enables continuous observation of clustering behavior of inclusions before and after the calcium treatment. Results show that the increase in average inclusion size in non-calcium-treated condition was much faster compared to calcium-treated condition. Results also show that the magnitude of attractive capillary force between inclusion particles in non-treated condition was about 10^{-15} N for larger particles (10 μm) and 10^{-16} N for smaller particles (5 μm) and acting length of force was about 30 μm. In the case of calcium-treated condition, the magnitude and acting length of force was reduced to 10^{-16} N and 10 μm, respectively, for particles of all sizes. This change in attractive capillary attractive force is due to change in inclusion morphology from solid alumina disks to liquid lens particles during calcium treatment.

DOI: 10.1007/s11663-017-0956-2

The demand for clean steel production is increasing in engineering industries to produce ultra-clean steels with superior mechanical and performance properties for various structural applications. Non-metallic inclusions in steel are harmful as they cause nozzle clogging during steel processing and also deteriorate the mechanical and performance properties of the final product.[1–3] During secondary steel making process, steel is de-oxidized with aluminum which results in the formation of alumina inclusions in steel. While small inclusions are less harmful, large inclusions can often be detrimental. They are sites for crack initiation. They also hinder performance in final products through reduced mechanical strength, toughness, corrosion resistance, and surface quality. In general, inclusions are removed by absorption into ladle slag during secondary steel making process. Since removal of all inclusions is not possible, residual inclusions are treated with calcium wire injection in molten steel which results in transforming solid alumina inclusions to liquid calcium aluminate inclusions, which helps in preventing the nozzle clogging.[4–6] Further, the mechanical properties of calcium-treated steel are improved in comparison to non-treated steels. Understanding inclusions morphology, distribution, and their agglomeration behavior is essential to further improve steel cleanliness and mechanical properties of the steel. However, several research studies were performed in the past to understand the effect of calcium treatment on morphological changes of oxide inclusions in steels, but still there is lack of information on understanding of clustering behavior and kinetics agglomeration of inclusions before and after calcium treatment.[6–8] Since steel is a high-temperature material, studying the clustering behavior of non-metallic inclusions in molten steel is a very challenging task. Confocal microscopy is an excellent technique which enables *in situ* observation of phase transformations at high temperatures in metallic alloys such steels, titanium, and nickel alloys.[9–11] HT-CSLM has been used by several researchers to investigate the agglomeration behavior of alumina inclusions in molten steel.[12–15] However, all these studies involved performing two experiments using two different samples collected from steel plants; one sample after aluminum killing of steel and the other after calcium treatment of aluminum killed steel. For the first time, we present *in situ* observation of calcium treatment of inclusions in liquid steel and their clustering behavior using HT-CSLM.

Al killed steel with composition (in wt. pct) 0.16 pct C, 0.67 pct Mn, 0.011 pct P, 0.012 pct S, 0.23 pct Si, and 0.027 pct Al was machined into a 2 mm cube. The cube was drilled to create an indent of 0.5-mm deep, which was subsequently packed with CaO powder. The sample was then placed inside an alumina crucible, contained within a Pt crucible and lid. Thereafter, it was placed on an alumina spacer to prevent sticking to the Pt sample stage. Figure 1(a) shows the sample set-up used in HT-CSLM.

The *in situ* experiment is designed in such a way that it is possible to heat the sample to a particular temperature and melt it partially while keeping the core solid which enables us to observe the agglomeration behavior of inclusions before reaction with CaO takes place. Later, this is followed by an increase in temperature so that the sample is fully molten and inclusions react with CaO.

BHARAT KHURANA and GOUR GOPAL ROY are with the Department of Metallurgical Engineering, Indian Institute of Technology, Kharagpur, West Bengal, 721302, India. STEPHEN SPOONER and PRAKASH SRIRANGAM are with WMG, University of Warwick, Coventry, Warwickshire, CV4 7AL, UK. M.B.V. RAO is with the R&D Department, Visakhapatnam Steel Plant, Visakhapatnam, Andhra Pradesh, 530031, India. Contact e-mail: P.srirangam@warwick.ac.uk

Manuscript submitted 13 September, 2016.
Article published online March 9, 2017.

The direction of sample melting as depicted in Figure 1(a) is integral to the experimental technique. The fraction of sample melted at different temperatures was calibrated and the direction of melting was deduced by heating dummy samples of identical dimensions to different temperatures [(1863 K, 1866 K, 1869 K, 1873 K, and 1876 K) (1590 °C, 1593 °C, 1596 °C, 1600 °C, and 1603 °C)]. While three-fourth of the sample was molten at a calibrated temperature of 1873 K (1600 °C), the sample was fully molten at a calibrated temperature of 1876 K (1603 °C). With information obtained from calibration samples, the actual experiment was performed. The experimental chamber was evacuated and refilled with argon (<2 ppm O_2) three times to remove any impurities from sample surface. The sample was heated to a calibrated temperature of 1873 K (1600 °C) under argon gas. The argon gas was then switched off so that the surface became still to observe the sample. After 30 seconds of observation in this condition, temperature was increased by 276 K (3 °C) to allow complete melting to facilitate reaction with CaO. Evolution of gas from the sample surface accompanied the reaction. Further description of CSLM experimental procedure can be found in Reference 16 Figure 1(b) shows a part of the frame observed after the sample was fully molten. The measurements and statistics of particle size, number, and distances were carried out through manual image analysis. The number of inclusions were counted through the recognition of inclusion appearance in the image; while particle sizes and pair distances are reported as a mean average of between 20 to 50 individuals and 10 to 20 pairings, respectively.

Figure 2 represents the variation of inter-inclusion distance as a function of time before and after calcium treatment. As shown in Figure 2(a), it is evident that before calcium treatment, the inter-inclusion distance decreases rapidly with time and eventually two inclusions merge together to form a cluster, while after the treatment, there is no significant change in inter-inclusion distance even after 6 seconds and much longer times are required for inclusions to form agglomerates as shown in Figure 2(b).

Figure 3(a) shows the variation of inclusion size with time. Initially, the inclusion particles at surface attracted each other from a distance much larger than their size. The size of inclusion particles increased rapidly with time which can be explained by agglomeration to form clusters. About 30 seconds later, surface flow due to the evolution of gas during calcium treatment caused the large inclusion clusters to go out of the field of view. However, soon after the calcium reaction was over, surface flow dampened and small inclusion particles surfaced, whose agglomeration behavior was then observed. As evident from Figure 3(a), the rate of increase in inclusion size was significantly reduced after calcium treatment. Figure 3(b) shows the variation of number of inclusions with time. The decrease in the number of inclusions was quite rapid initially, but slowed down after calcium treatment. (Note: For after calcium treatment condition in Figure 3b, time $t = 0$ seconds has been taken to be the moment when gas evolution due to reaction with calcium is observed).

Figure 4(a) shows the variation of inter-inclusion distance as a function of time for a pair of inclusion particles observed just after melting of sample and those observed 5, 20, and 30 seconds later. Figure 4(b) shows the variation of inter-inclusion distance as a function of time for pairs of inclusion particles observed 5, 20, 30, and 60 seconds after calcium treatment. For before calcium treatment condition, drastic decrease in inter-inclusion distance was observed once the interparticle distance was 30-35 μm. It indicates that a long-range attraction force was operating between the particles. But, after calcium treatment, a slowdown in agglomeration of inclusions was observed, indicating a change in the mechanism of agglomeration. The change was not visible immediately. But, 20 seconds after the treatment, a significant slowdown in agglomeration of inclusions could be observed. Magnitude and acting length of force operating between inclusion particles was calculated using the method discussed in greater detail elsewhere.[13] The particle shape was assumed to be elliptical, and the lengths of long axis and short axis of a particle were observed. Height of elliptical disks was taken to be 2 μm on the basis of confocal observations by Yin *et al.****[12] Density of inclusions was taken to be 3000 Kg m^{-3}. Before calcium treatment, the magnitude of the force was 9.911×10^{-16} N for a pair of inclusion

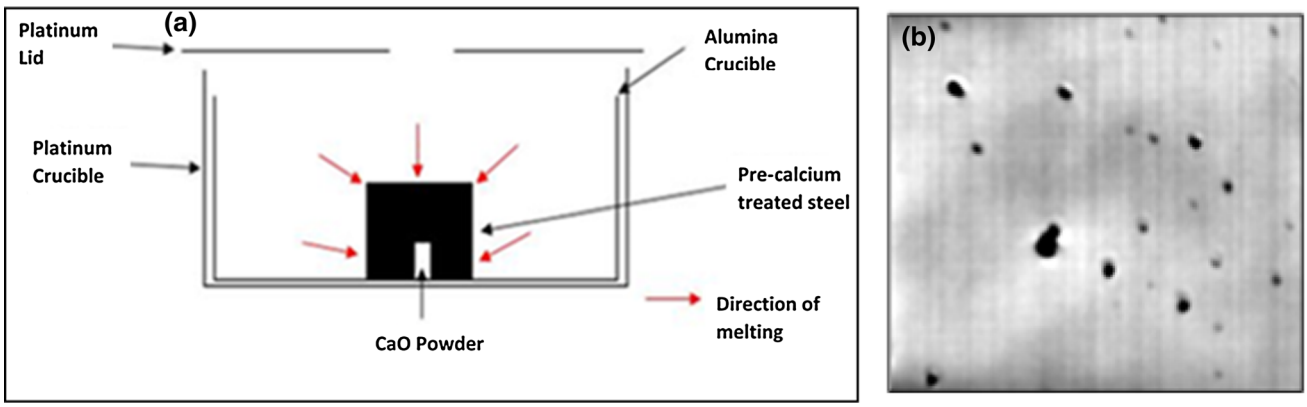

Fig. 1—(*a*) Schematic of the experimental set-up, designed to offer minimal surface flow, and allow for partial melting of the sample (*b*) Surface view of the sample soon after melting.

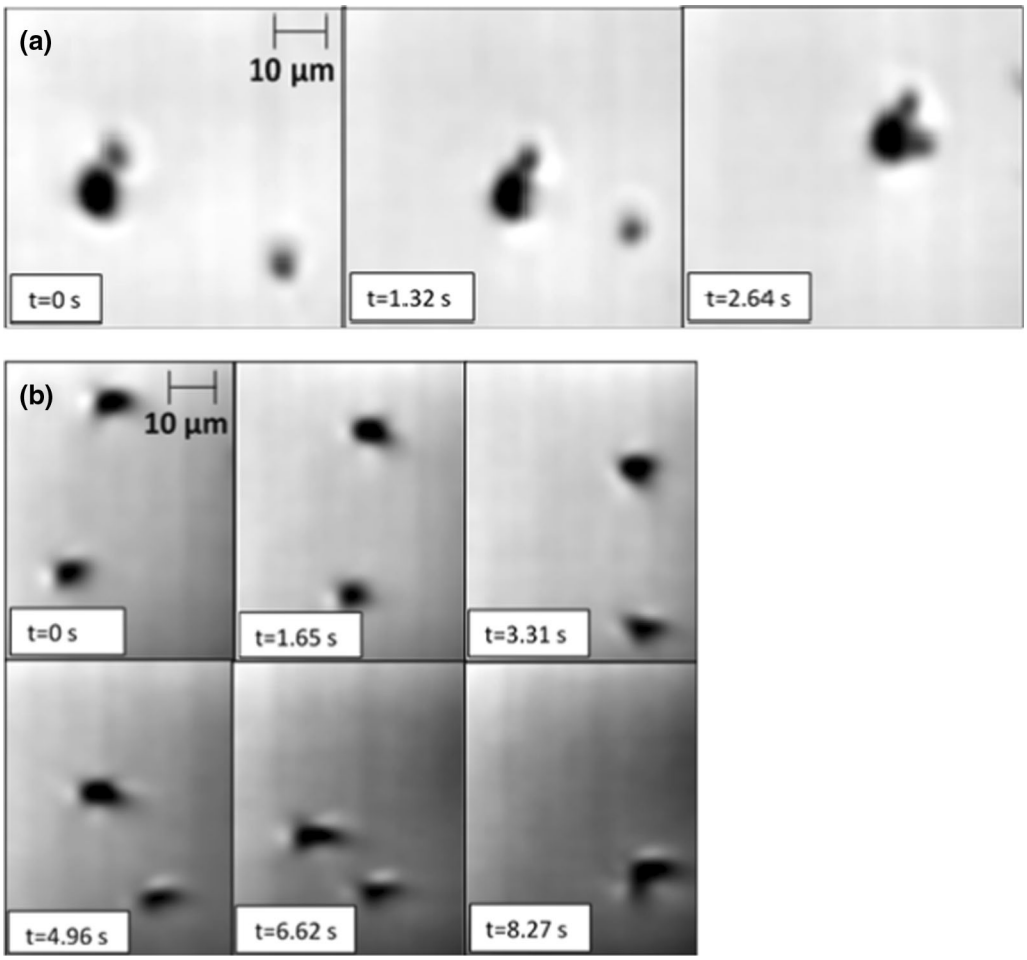

Fig. 2—Change in inter-inclusion distance with time for a pair of inclusion particles observed (*a*) Before calcium treatment (*b*) After calcium treatment.

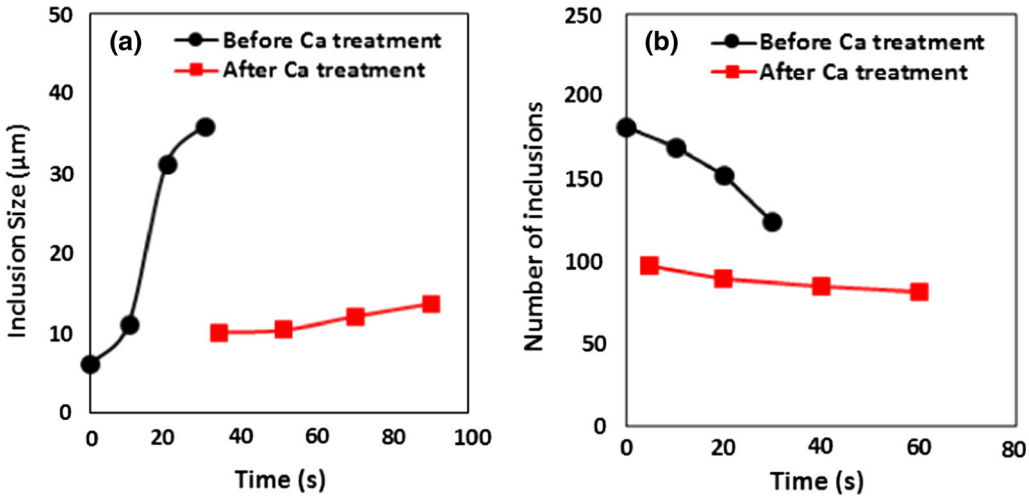

Fig. 3—Variation of (*a*) Inclusion size (*b*) Number of inclusions with holding time during confocal microscopy.

particles with size 10 μm each and 5.476 × 10^{-16} N for a pair of inclusion particles with size 5 μm each and the acting length of force was 30 μm. After calcium treatment, magnitude and acting length of force was reduced to 10 $^{-16}$ N and 10 μm, respectively, for particles of all sizes. Similar studies were performed by Salgado *et al.* using two different samples, one, calcium treated and the other non-treated.[14] They have reported an attractive

force value of 10^{-16} to 10^{-15} N for calcium-treated sample and 10^{-15} to 10^{-14} N for non-treated sample which is in close agreement with our results. Reduction in magnitude and acting length of force after calcium treatment is considered to be responsible for change in agglomeration behavior of inclusions.

In order to identify the type of inclusions and their morphology in steel before and after calcium treatment, we have performed SEM studies on the sample after *in situ* confocal study. Figure 5 shows the SEM in-line detector image of an alumina inclusion in the original stock steel before treatment. It can be seen from the image that several crystal-like features are apparent and an elongated morphology is apparent. There is confirmation through EDS of the enrichment of aluminum and oxygen in this area, and no increased levels of calcium or sulfur are present.

Figure 6 represents SEM in-line detector image of a inclusion in steel after calcium treatment. As shown from the EDS mapping, it is clear that the inclusion is enriched in aluminum, oxygen, calcium, and sulfur. It has previously been reported[5,7,17] that calcium-treated inclusions display a ring of sulfur enrichment around the inclusion, as this sample is taken straight from the CSLM to the SEM without sectioning or polishing, the analysis is from a completely external view point (not the cross-sectional view of a treated inclusion that would show the traditionally reported sulfur ring) and as such the enriched calcium sulfide layer appears across the entire sample, as the "crus" has not been broken. The image shows a much more circular geometry compared to the before treatment sample inclusion which would coincide with the change to a liquid phase in the samples life cycle before quenching.

The change in magnitude of force operating between a pair of inclusion particles can be explained by their morphology.[13] Alumina inclusions take the shape of disk on the inert gas/molten steel interface and the angle of contact at the interface between alumina inclusion and molten steel is 133 deg.[12] When two alumina inclusions come close to each other, there is a depression of inert gas/molten steel interface between them. It results in a difference in pressure on two sides of inclusion particle because of molten steel on one side and inert gas on the other side. This pushes the inclusion particles toward each other. However, after calcium treatment, calcium aluminate inclusions are formed. Their composition as determined using an SEM–EDS indicates that they are liquid/semi-liquid at 1873 K (1600 °C). These inclusions take the shape of lens-like particles on the inert gas/molten steel interface.[13] The depression of inert gas/molten steel interface when such lens-like particles come close to each other is much lesser, resulting in a significantly weaker force of attraction and reduced acting length of force. On the basis of morphology of particles, the force of attraction is expected to follow the order: Liquid/liquid pair < liquid/semi-liquid pair < semi-liquid/semi-liquid pair < liquid/solid pair < semi-liquid/solid pair < solid/solid pair. The reason for this order is that the contact angle between solid inclusion particles and molten steel is greater than 90 deg, and hence when two such particles come close to each other, there is a depression of the gas/molten steel interface between them. The pressure difference on either side of the inclusions causes the liquid steel to push the two inclusion particles toward each other. However, due to different morphology of semi-solid inclusion particles, the depression of the gas/molten steel interface is reduced in comparison when a semi-solid particle and a solid particle come close to each other. Liquid inclusion particles take lens-like shape on the surface of molten steel.[12,13] Thus, the depression of interface is much lower when two

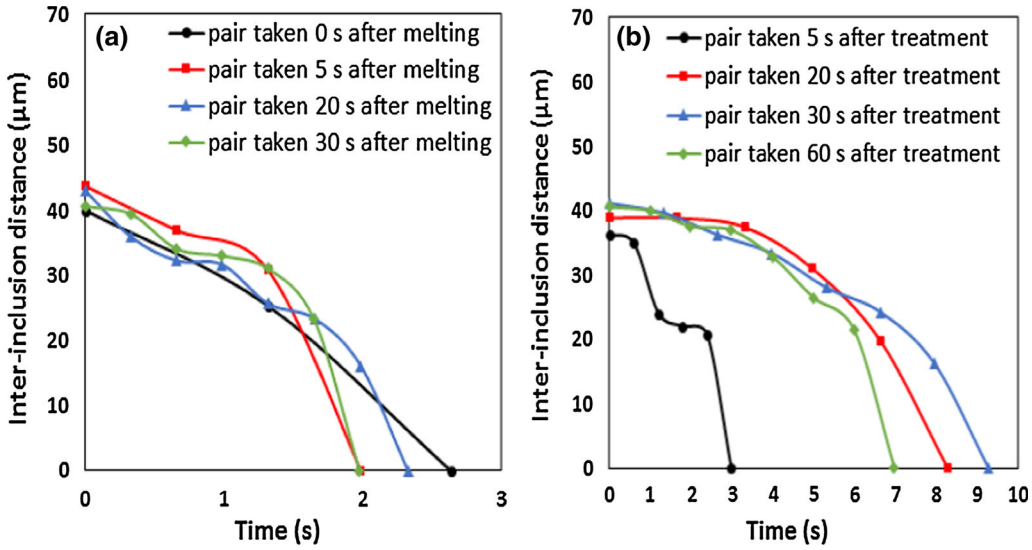

Fig. 4—Variation of inter-inclusion distance as a function of time for different pairs of inclusion particles observed (*a*) 0, 5, 20, and 30 s after melting of sample (*b*) 5, 20, 30, and 60 s after Ca treatment.

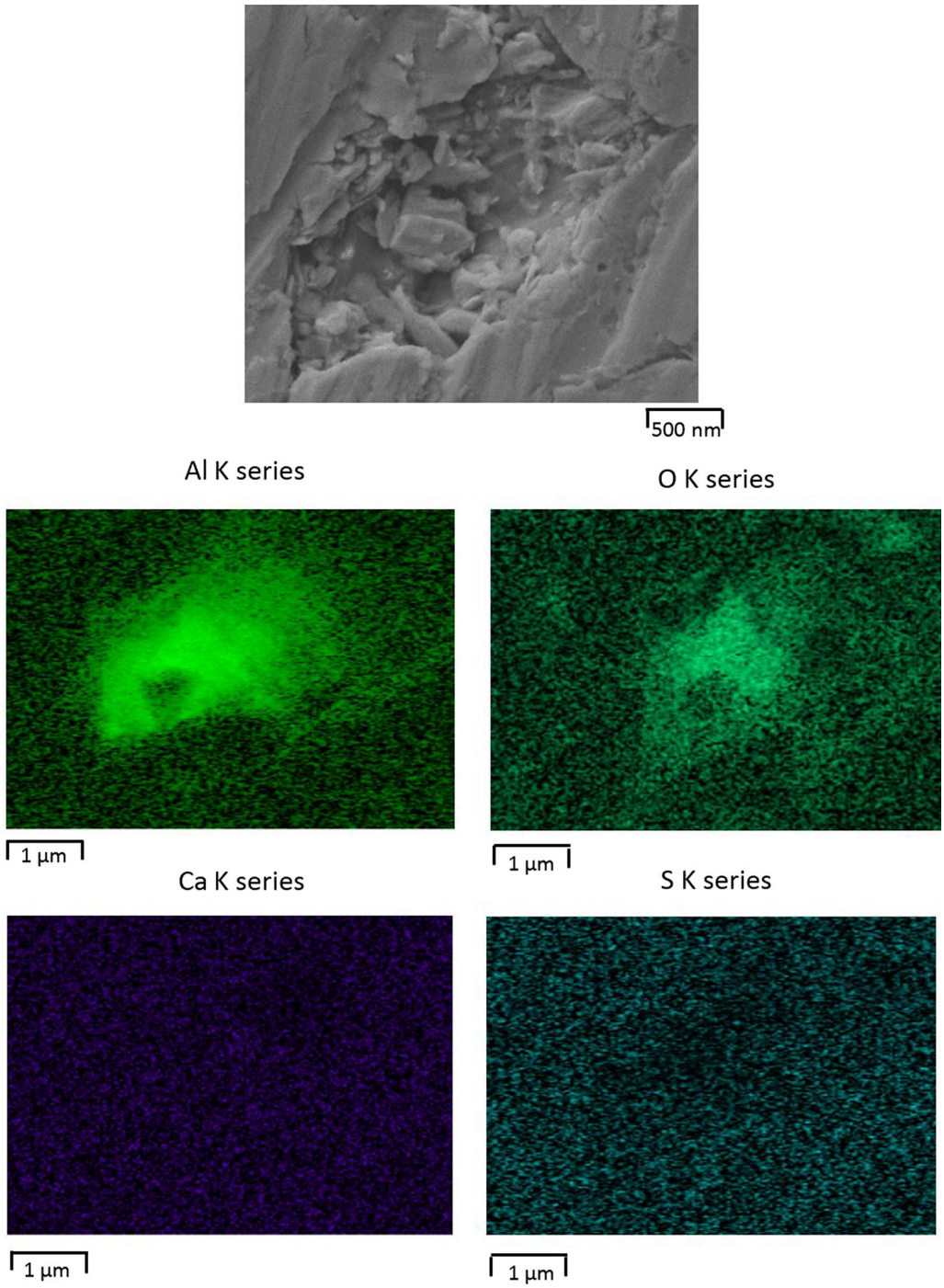

Fig. 5—SEM–EDS image and chemical mapping for an inclusion observed in the before treatment material.

liquid particles come close to each other, resulting in a much weaker capillary force acting to cause agglomeration.

Calcium treatment of inclusions in liquid steel is an important part of secondary steel making. Alumina inclusions in molten steel are solid disk-like particles which tend to agglomerate and form clusters leading to nozzles getting clogged. Calcium treatment results in change of these alumina inclusions to liquid calcium aluminate inclusions which have reduced agglomeration tendency and hence do not cause nozzle clogging. The present study tries to simulate the process of calcium treatment (as well as the possible treatment with CaO) in industry using a sample obtained from the ladle furnace prior to calcium treatment. The sample was melted and treated with calcium oxide powder and *in situ* observations were made on agglomeration behavior of inclusions before and after treatment using confocal

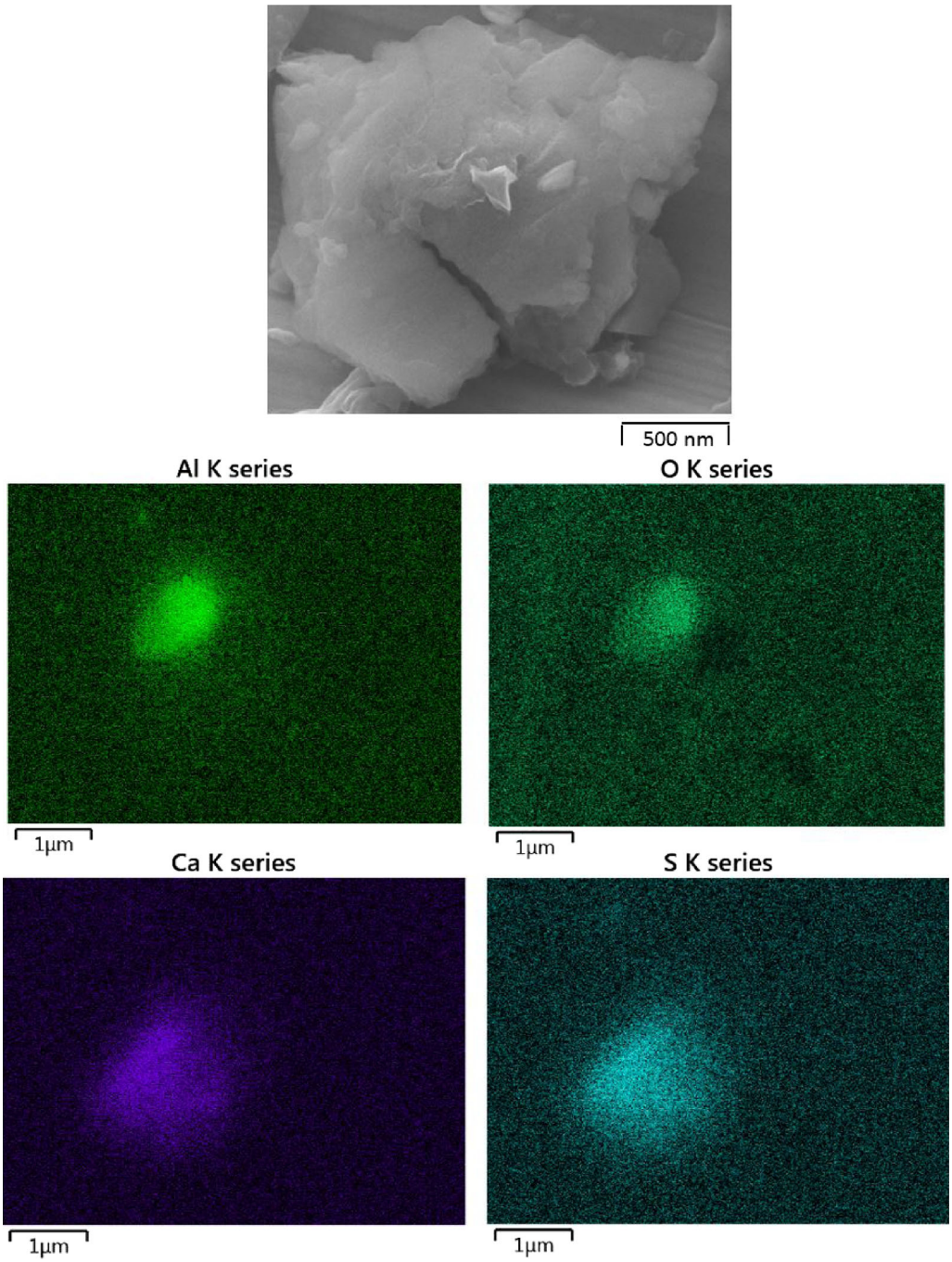

Fig. 6—SEM–EDS image and chemical mapping for an inclusion observed on the surface of the sample after calcium treatment.

microscopy. The findings of the present study are as follows:

- It was observed that prior to calcium treatment, average inclusion size increased due to clustering from 6.17 to 35.97 μm in 30 seconds but after calcium treatment it increased only slightly from 10.1 to 13.67 μm even after a holding time of 60 seconds.
- Results show that for the same initial inter-inclusion distance of about 40 μm, a pair of inclusion particles before calcium treatment took 2.6 seconds to come together while a pair of inclusion particles after calcium treatment took more than 8 seconds to come together.
- From the present study, it can be concluded that after calcium treatment, magnitude and acting length of force responsible for agglomeration of inclusions reduced causing a delay in the collision and clustering of inclusion particles as compared to before treatment. The rate of this effect from the initial point of treat-

ment in a continuous experiment has also been reported for the first time in this manner alluding to initial reaction kinetics.

The authors would like to thank Professor Sridhar Seetharaman and Dr. Michael Auinger at University of Warwick for their fruitful discussions during preparation of the manuscript.

REFERENCES

1. H.V. Atkinson and G. Shi: *Prog. Mater. Sci.*, 2003, vol. 48, pp. 457–520.
2. R.B. Tuttle, J.D. Smith, and K.D. Peaslee: *Metall. Mater. Trans.*, 2005, vol. 36B, pp. 885–92.
3. P. Misra, V. Chevrier, S. Sridhar, and A.W. Cramb: *Metall. Mater. Trans.*, 2000, vol. 31B, pp. 1135–39.
4. Y. Wang, M. Valdez, and S. Sridhar: *Metall. Mater. Trans.*, 2002, vol. 33B, pp. 625–32.
5. N. Verma, P.C. Pistorius, R.J. Fruehan, M. Potter, M. Lind, and S. Story: *Metall. Mater. Trans.*, 2011, vol. 42B, pp. 711–19.
6. Y. Kang, B. Sahebkar, P.R. Scheller, K. Morita, and D. Sichen: *Metall. Mater. Trans.*, 2011, vol. 42B, pp. 522–34.
7. L. Zhang and B.G. Thomas: *Metall. Mater. Trans.*, 2006, vol. 37B, pp. 733–61.
8. C. Blais, G.L. Esperance, H. Lehuy, and C. Forget: *Mater. Charact.*, 1997, vol. 38, pp. 25–37.
9. M.M. Attallah, H. Terasaki, R.J. Moat, S.E. Bray, Y. Komizo, and M. Preuss: *Mater. Charact.*, 2011, vol. 62, pp. 760–67.
10. L. Deillon, J. Zollinger, D. Daloz, M. Založnik, and H. Combeau: *Mater. Charact.*, 2014, vol. 97, pp. 125–31.
11. M. Reid, D. Phelan, and R. Dippenaar: *Metall. Mater. Trans.*, 2004, vol. 44B, pp. 565–72.
12. H. Yin and H. Shibata: *ISIJ Int.*, 1997, vol. 37, pp. 936–45.
13. T. Emi, M. Suzukl, H. Yin, and H. Shibata: *ISIJ Int.*, 1997, vol. 37, pp. 946–55.
14. U. Diéguez-Salgado, S. Michelic, and C. Bernhard: *IOP Conf. Ser. : Mater. Sci. Eng.*, 2016, vol. 119, Conference 1.
15. B. Coletti, S. Vantilt, B. Blanpain, and S. Sridhar: *Metall. Mater. Trans*, 2003, vol. 34B, pp. 533–38.
16. A.N. Assis, J. Warnett, S. Spooner, R.J. Fruehan, M.A. Williams, and S. Sridhar: *Metall. Mater. Trans.*, 2014, vol. 46B, pp. 568–76.
17. D. Zhao, H. Li, C. Bao, and J. Yang: *ISIJ Int.*, 2015, vol. 55, pp. 2115–24.